

In these equations Lagrange multipliers are defined as follows:

$$\gamma^M = -(\gamma^M)^T, \quad \gamma^C = -(\gamma^C)^T, \quad \gamma^K = -(\gamma^K)^T \quad (10)$$

Minimization and simplification results in a set of homogeneous linear equations

$$\begin{aligned} ML_1 + L_1M + CL_2 + L_2^T C + KL_3 + L_3^T K &= 0 \\ ML_2^T + L_2M + CL_4 + L_4C + KL_5 + L_5^T K &= 0 \\ ML_3^T + L_3M + CL_5^T + L_5C + KL_6 + L_6K &= 0 \end{aligned} \quad (11)$$

where

$$\begin{aligned} L_1 &= \text{Re}(UU^*), \quad L_2 = \text{Re}(VU^*), \quad L_3 = \text{Re}(WU^*) \\ L_4 &= \text{Re}(VV^*), \quad L_5 = \text{Re}(WV^*), \quad L_6 = \text{Re}(WW^*) \end{aligned} \quad (12)$$

and an asterisk denotes complex conjugate transpose.

To obtain a nontrivial solution, however, at least one nonzero element of any one of the matrices M , C , and K must be specified. If this condition is satisfied, the set of equations in Eq. (11) can be solved by neglecting the rows obtained by differentiating β with respect to the known elements and substituting the values of these elements into the remaining equations, thus converting the system into an inhomogeneous one. If the total mass of the system is known and if the mass matrix is assumed to be diagonal, the preceding procedure can be used to get a unique solution. This is accomplished by first assigning an arbitrary value to one of the elements of the diagonal mass matrix and solving for the remaining unknowns in M , C , and K . The identified matrices are then multiplied by a scalar so that the sum of the diagonal elements of the revised mass matrix is equal to the total mass and the ratios between the diagonal elements are preserved.

Numerical Results

As a first step, the performance of the described identification method is evaluated by assuming a set of M , C , K and determining the eigenvalues and eigenvectors which in turn are treated as experimental data in the identification procedure. A comparison of the identified and assumed M , C , K (Table 1) for a simple case involving nonproportional damping illustrates satisfactory performance. Damping values that are not present in most a priori models are estimated in this procedure. As a second example, a cantilever beam (Fig. 1) is considered. Experimentally, eigenvalues and eigenvectors have been determined at three locations. A corresponding three DOF a priori finite element model has been constructed from a larger DOF finite element model and Guyan reduction method. Identification procedure has then been applied by first assuming that the entire mass matrix is known and equal to the a priori mass matrix (case 1). The generated experimental data constitute the input to the procedure. Later, the identification procedure has been repeated by using only the diagonal elements of the a priori matrix as known (case 2). A comparison of the results is illustrated in Tables 2 and 3. A simulation to a high degree of accuracy in case 2 is attributed to the increased freedom available in adjusting the system matrices especially where experimental data are available at relatively fewer degrees of freedom.

Cases in which experimental data are not available for all the modes were investigated by considering the test results for higher modes as unknown. A priori analytical modal parameters were substituted for the higher modes for which experimental data were assumed to be lacking. As before, the model identified in each case using a priori diagonal

mass elements was found to reproduce the specified modal parameters very accurately.

In some cases where some of the coefficients of the stiffness matrix were assumed to be known a priori and the coefficients of the mass and damping matrices were identified, the results were not always satisfactory. Even though the matrices obtained satisfied the equations of the eigenvalue problem, they were found not to be positive-definite, which would be considered unacceptable for most physical systems.

Conclusions

An identification procedure has been developed to estimate the mass, damping, and stiffness matrices from experimental eigenvalues and eigenvectors. The method is based on the minimization of the eigenvalue equation error subject to the conditions of symmetry of the matrices involved. If one or more nonzero coefficients in any of the matrices are given, the remaining coefficients in all the matrices can be found. The identified matrices are symmetric and satisfy the eigenvalue problem as accurately as possible. The method is applicable in all cases of damping, either proportional or nonproportional. Example problems are solved to indicate the validity of the approach. Results obtained in these examples also demonstrate that the procedure is capable of identifying systems that simulate experimental modal data to high levels of accuracy (when diagonal elements of the mass matrix were assumed to be known a priori). Application of the technique to systems with large degrees of freedom is still to be evaluated.

Acknowledgment

Authors gratefully acknowledge support for this work from U.S. Army Research Contract DAAG 29-82-K-0094.

References

- ¹Caravani, P., Watson, M. L., and Thomson, W. T., "Recursive Least-Squares Time Domain Identification of Structural Parameters," *Journal of Applied Mechanics*, Vol. 44, March 1977, pp. 135-140.
- ²Kozin, F. and Kozin, C. H., "Identification of Linear Systems, Final Report on Simulation Studies," NASA CR-98738, April 1968.
- ³Yun, C. B. and Shinozuka, M., "Identification of Nonlinear Structural Dynamic Systems," *Journal of Structural Mechanics*, Vol. 8, 1980, pp. 187-203.
- ⁴Caravani, P. and Thomson, W. T., "Identification of Damping Coefficients in Multidimensional Linear Systems," *Journal of Applied Mechanics*, Vol. 41, June 1974, pp. 379-382.
- ⁵Beliveau, J. G., "Identification of Viscous Damping in Structures from Modal Information," *Journal of Applied Mechanics*, Vol. 43, June 1976, pp. 335-339.
- ⁶Ibrahim, S. R., "Dynamic Modeling of Structures from Measured Complex Modes," AIAA Paper 82-0770.

Postbuckling of Thick Circular Plates with Edges Restrained Against Rotation

K. Kanaka Raju* and G. Venkateswara Rao*
Vikram Sarabhai Space Center, Trivandrum, India

Introduction

THE continuum finite-element formulations for the postbuckling analysis of circular plates is given in Ref. 1. A direct and simple finite-element formulation to study the

Received Jan. 17, 1986; revision received April 15, 1986. Copyright © American Institute of Aeronautics and Astronautics, Inc., 1986. All rights reserved.

*Scientist/Engineer, Structural Engineering Group.

same problem, is proposed in Ref. 2, wherein only simply supported and clamped boundary conditions on the plate are considered. However, the practical boundary conditions are more appropriately described by introducing a rotational spring at the edge of the plate. The normally used simply supported and clamped boundary conditions* can be achieved from the limiting values of the rotational spring stiffness.

The effect of a rotational spring at the edge of the plate on the postbuckling behavior of thin circular plates is studied in Ref. 3.

However, for moderately thick circular plates with elastic edge rotational restraints, the new finite-element formulation of Refs. 2 and 3 has to be modified to include the effect of the shear deformation. The postbuckling behavior of such plates is studied here for the first time in the literature. The finite-element formulation is touched upon briefly and a set of numerical results are presented for various values of the rotational spring stiffness and the thickness of the plate.

Finite-Element Formulation

The strain displacement relations of a moderately thick circular plate under axisymmetric conditions are given by

$$\begin{aligned}\epsilon_r &= \frac{du}{dr} + \frac{1}{2} \left(\frac{dw}{dr} \right)^2 \\ \epsilon_\theta &= u/r \quad \epsilon_{rz} = -\zeta \\ \chi_r &= - \left(\frac{d^2 w}{dr^2} + \frac{d\zeta}{dr} \right) \quad \chi_\theta = - \frac{1}{r} \left(\frac{dw}{dr} + \zeta \right)\end{aligned}\quad (1)$$

where ϵ_r , ϵ_θ and ϵ_{rz} are the strains, χ_r and χ_θ are the curvatures, u and w the radial and lateral displacements, ζ the shear rotation, and r , θ , and z the radial, circumferential, and lateral directions, respectively.

The circular plate of radius a is discretized into a number of annular plate elements and the strain energy U of an element bounded by radii r_1 and r_2 is given by

$$\begin{aligned}U &= \frac{1}{2} \int_0^{2\pi} \int_{r_1}^{r_2} \left[C \left(\epsilon_r^2 + \epsilon_\theta^2 + 2\nu\epsilon_r\epsilon_\theta \right) \right. \\ &\quad + D \left(\chi_r^2 + \chi_\theta^2 + 2\nu\chi_r\chi_\theta \right) + \frac{5}{6} G h \epsilon_{rz}^2 \Big] r dr d\theta \\ &\quad + K_s a \pi \left(\frac{dw}{dr} + \zeta \right)^2 \Big|_{r=a}\end{aligned}\quad (2)$$

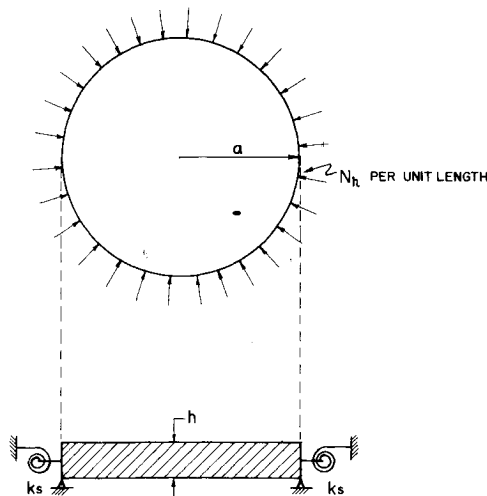


Fig. 1 Moderately thick circular plate with the edge elastically restrained against rotation.

It is to be noted that the term due to the rotational spring stiffness K_s in Eq. (2) contributes to the strain energy of the element at the boundary of the plate only. In Eq. (2), h is the thickness of the plate, $C = Eh/(1 - \nu^2)$ and $D = Eh^3/12(1 - \nu^2)$, E being the Young's modulus, ν the Poisson's ratio (taken as 0.3 in the present study), and G the shear modulus given by $G = E/2(1 + \nu)$.

The work done on the element by the compressive load N_r per unit length at the boundary is given by

$$W = \frac{1}{2} \int_0^{2\pi} \int_{r_1}^{r_2} N_r \left(\frac{dw}{dr} \right)^2 r dr d\theta \quad (3)$$

Following standard principles⁴ with cubic displacement distributions in r assumed for u , w , and ζ (the degrees of freedom being u , du/dr , w , dw/dr , ζ , and $d\zeta/dr$, the final matrix equation governing the postbuckling behavior is obtained as

$$[K] \{\delta\} + \lambda [G] \{\delta\} = 0 \quad (4)$$

where $[K]$ and $[G]$ are the assembled elastic and geometric stiffness matrices, respectively, $\{\delta\}$ the eigenvector, and λ the eigenvalue.

The iterative numerical method of Ref. 3 is used to evaluate the nonlinear stiffness matrix $[K]$ and to solve Eq. (4) to obtain the linear buckling load parameter λ_L (defined as, $\lambda_L = (N_{r,cr} a^2)/D$, where $N_{r,cr}$ is the critical radial load) and the postbuckling radial load parameter λ_{NL} (defined as $\lambda_{NL} = N_r a^2/D$) for a given central lateral deflection c .

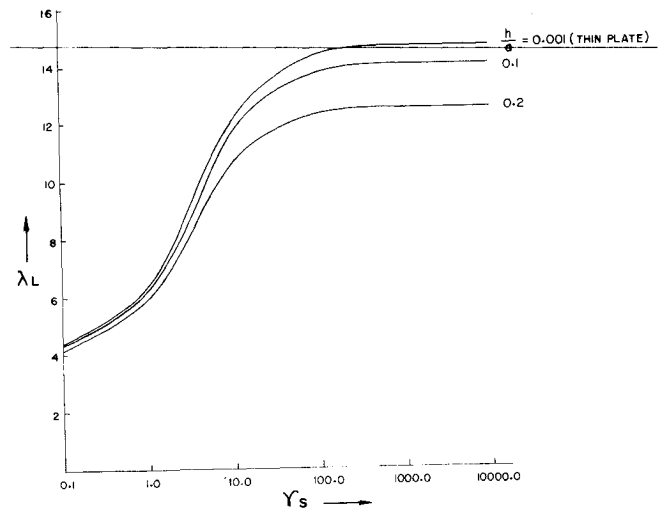


Fig. 2 Variation of λ_L with γ_s .

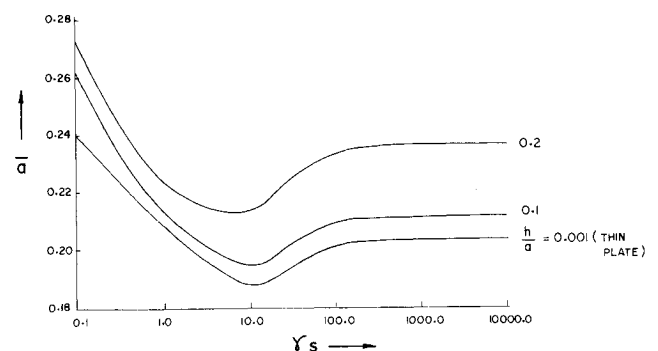


Fig. 3 Variation of \bar{a} with γ_s .

Numerical Method

Equation (4) is solved by an iterative method with the following steps:

1) The stiffness matrix $[K]$ is obtained in the first step by neglecting all the nonlinear terms, which yields the linear stiffness matrix $[K_L]$. Using $[K_L]$ and $[G]$, the linear critical load parameter λ_L and linear eigenvector $\{\delta_L\}$ are obtained from Eq. (4).

2) The onset of postbuckling occurs when the plate undergoes a lateral deflection for a given radial load parameter λ_{NL} , with λ_{NL} just greater than λ_L . λ_{NL} is computed as follows: for a specified maximum lateral central deflection c , the linear eigenvector $\{\delta_L\}$ is scaled up by c times so that the resulting vector will have a lateral displacement c at the maximum deflection point.

3) Using the scaled up eigenvector, the nonlinear terms in the stiffness matrix $[K]$ are obtained through numerical integration.

4) Using the new $[K]$ and $[G]$ and treating the problem as a linear eigenvalue problem, the radial load parameter λ_{NL} and the nonlinear eigenvector $\{\delta_{NL}\}$ are obtained.

5) Steps 2-4 are repeated by replacing $\{\delta_L\}$ with $\{\delta_{NL}\}$ in step 2 to obtain a converged radial load parameter to the prescribed accuracy, say 10^{-4} .

6) Steps 1-5 are repeated for various values of c .

Numerical Results and Discussion

The above formulation is employed to obtain λ_L and λ_{NL} values of moderately thick circular plates with the thickness ratio h/a varying between 0.001 (thin plate) and 0.2 with edges elastically restrained against rotation. (See Fig. 1.) The spring stiffness parameter γ_s (defined as $\gamma_s = K_s a/D$) is considered to vary from 0.0 (simply supported) to 10,000.0 (clamped). λ_{NL} values are presented in this Note in the form of radial load ratio λ defined as

$$\gamma = \frac{\lambda_{NL}}{\lambda_L} = \frac{N_r}{N_{cr}}$$

for which an empirical formula is obtained through a least square curve fitting technique as

$$\gamma = 1 + \bar{a}(c/h)^2 - \bar{b}(c/h)^4 \quad (5)$$

from the γ values obtained for various values of c/h (ranging 0.0-1.0 in steps of 0.2), where c is the central deflection of the plate.

It is found that, by a convergence study with four and eight-element idealization of the plate for an extreme case of $h/a=0.2$, the eight-element solution is very accurate and, hence, all further computations are carried out with an eight-

element idealization. Also, it is observed that in Eq. (5), $\bar{b} \ll \bar{a}$ and the variation of γ is predominantly determined by the variation of \bar{a} for c/h values of practical interest. Hence, without loss of accuracy, γ can be written as

$$\gamma = 1 + \bar{a}(c/h)^2 \quad (6)$$

The extreme cases of spring stiffness namely 0.0 and a value above 1000.0 represent the usual simply supported and clamped conditions at the edge. For h/a values of 0.001, 0.1, and 0.2, the λ_L and \bar{a} values for $\gamma_s=0.0$ are 4.198, 4.148, 4.006 and 0.2702, 0.2734, 0.2831, respectively. For $\gamma_s=10,000.0$, the corresponding values are 14.68, 14.09, 12.57 and 0.2028, 0.2112, 0.2363.

The variation of λ_L and \bar{a} with the spring stiffness parameter γ_s are presented in Figs. 2 and 3 respectively, for h/a values of 0.001, 0.1, and 0.2. From these figures the following broad observations can be made:

1) For a given h/a , λ_L increases as γ_s increases up to a value of about 1000 and remains constant thereafter.

2) For a given γ_s , λ_L decreases as h/a increases.

3) For a given h/a , \bar{a} first decreases as γ_s increases from 0.1 and then approaches a constant value for higher values of γ_s .

4) For a given γ_s , \bar{a} increases as h/a increases.

Conclusions

Postbuckling behavior of moderately thick circular plates with edges elastically restrained against rotation has been considered in this Note. It is observed that the radial load ratio for a plate with a particular thickness initially decreases as the spring stiffness increases from 0.0 (simply supported condition) and then increases to reach the clamped plate results when $\gamma_s=10,000.0$. Also, it is seen that the radial load ratio increases as the thickness of the plate increases for any particular spring stiffness value.

The formulation is quite general and can be employed for investigating postbuckling behavior of plates of any shape under any type of boundary conditions.

References

- Thomson, J.M.T. and Hunt, G.W., *A General Theory of Elastic Stability*, John Wiley & Sons, London, 1973, pp. 160-178.
- Rao, G.V. and Raju, K.K., "A Reinvestigation of Post-buckling Behavior of Elastic Circular Plates Using a Simple Finite Element Formulation," *Computers and Structures*, Vol. 17, 1983, pp. 233-236.
- Raju, K.K., and Rao, G.V., "Post-buckling of Cylindrically Orthotropic Circular Plates on Elastic Foundation with Edges Elastically Restrained against Rotation," *Computers and Structures*, Vol. 18, 1984, pp. 1183-1188.
- Zienkiewicz, O.C., *Finite Element Method in Engineering Science*, McGraw-Hill, New York, 1971.